JMEPEG (2010) 19:666–671
DOI: 10.1007/s11665-009-9535-2

1059-9495/$19.00

316L Stainless Steel with Gradient Porosity Fabricated by Selective Laser Melting

Ruidi Li, Jinhui Liu, Yusheng Shi, Mingzhang Du, and Zhan Xie

(Submitted March 18, 2009; in revised form July 7, 2009)

To fabricate 316L stainless steel part with a pore gradient structure, the method using selective laser melting (SLM) technique is exploited. Scan tracks feature, densification, and tensile property of SLM-produced samples prepared via different scan speeds were investigated. The results show that the porosity is strongly influenced by scan speed. On this basis, a gradient changed scan speed was applied in every SLM layer for the purpose of producing a gradient porosity metal. The results indicate that the structure exhibits a gradually increased porosity and a reduced molten pool size along the gradient direction of scan speed variation. The forming mechanisms for the gradient porosity were also addressed.

Keywords pore gradient, selective laser melting, 316L stainless steel

1. Introduction

Porous metals have been widely used in biomaterials, biochemistries, electronics, etc., owing to their outstanding properties (Ref 1). However, there are some problems in porous metal fabricated by present techniques, such as low controllability in porosities and performances. Moreover, it is difficult to fabricate porous metals with high porosities and high mechanical properties simultaneously (Ref 2), as higher porosity could deteriorate their mechanical performance. A material with a gradient porosity from higher to lower could lead to a gradual mechanical property variation from lower to higher. Thus, the gradient porosity material can be the ideal scheme in solving this problem. Currently, the reported methods for fabricating gradient porous materials include colloidal infiltration (Ref 3), electric field-assisted processing (Ref 4), powder sintering (Ref 5), etc. Nevertheless, such methods are not flexible in the porosity controllability and the net shaping.

Selective laser melting (SLM) is a relatively new rapid prototyping (RP) technique through which the three-dimensional metallic parts can be fabricated directly from computer aided design (CAD) data without using any traditional tooling (Ref 6-8). In this method, a high-energy laser is used to selectively fuse thin powder layers. Moreover, SLM technology is flexible in controlling porosities according to different laser energy inputs (Ref 9-11), showing a great potential for producing porous materials. Fortunately, Gu et al. have studied fabrication of porous metal using direct laser forming technology (Ref 12, 13). Moreover, they pointed out that the porosity of SLM-produced parts can be easily controlled by processing parameters. Therefore, SLM technology is promising in producing gradient porous metal by setting a gradient-varied parameter in every processing layer. In this article, we investigated into fabrication of the 316L stainless steel material with a gradient porosity via SLM technique.

Ruidi Li and **Yusheng Shi**, State Key Laboratory of Material Processing and Die & Mould Technology, Huazhong University of Science and Technology, Wuhan 430074, China; **Jinhui Liu**, Heilongjiang Institute of Science and Technology, Harbin 150027, China; and **Mingzhang Du** and **Zhan Xie**, Shichuan Petroleum Perforating Materials Ltd, Longchang 642177, China. Contact e-mails: lrdcsu@hotmail.com and shiyusheng@263.net.

2. Experimental

2.1 Materials

In this experiment, gas atomizing 800 mesh 316L stainless steel powder (99% purity) was used for SLM process. Figure 1 shows the morphologies of the 316L stainless steel powders. This powder exhibited a spherical morphology and a wide size distribution. Elemental compositions of this powder were: 16.7Cr, 12.8Ni, 2.8Mo, 2.4C, 0.9Si, 0.05Mn, and Fe balance.

2.2 Single-Layer Forming Process

In a single-layer forming process, the scan speeds vary from 90 to 180 mm/s with an increment of 30 mm/s. The laser power of 100 W, scan interval of 0.1 mm, and layer thickness of 0.06 mm were fixed as constants.

2.3 Multi-Layers Forming Process

In this experiment, a self-developed commercial HRPM-II SLM machine from Huazhong University of Science & Technology (HUST) was used. The system was equipped with a 100 W continuous wave fiber laser. The building chamber of this system could be vacuumed and protected by argon gas.

Figure 2 shows the multi-layers forming process of this experiment. In each fabricated layer, the variational mode of scan speed is identical. The multi-layers forming comprise

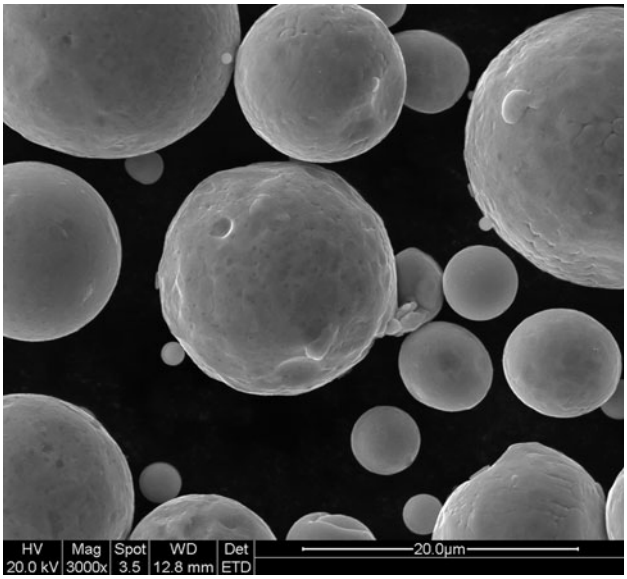

Fig. 1 SEM image showing morphologies of 316L stainless steel powders

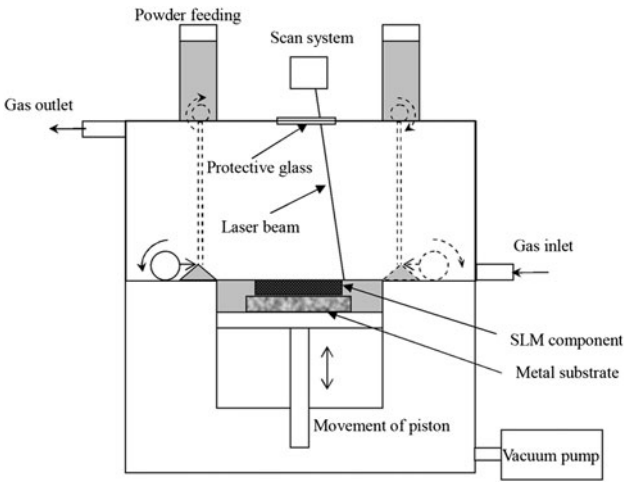

Fig. 2 Diagrammatic sketch for multi-layers forming process

three main steps: (1) a certain quantity of fresh powders is sent into working cylinder from powder feeding system, then a smooth powder layer with a certain thickness is produced via a roller; (2) the powders are melted and solidified rapidly by a high energy from fiber laser according to the single-layer forming method; and (3) the piston moves down a layer thickness, then the same action is repeated before a complete component can be formed. Thus, with the repeated single-layers forming process, a rectangular block with dimension of $15 \times 12 \times 1$ mm^3 was prepared, and a gradient porosity microstructure along the speed gradient direction was obtained. In addition, to evaluate the influence of scan speed on the porosity and mechanical property of SLM-prepared samples, separate samples were fabricated under different scan speeds.

2.4 Characterization

Finally, porosities of samples produced at different scan speeds were measured by Archimedes law. Then, tensile

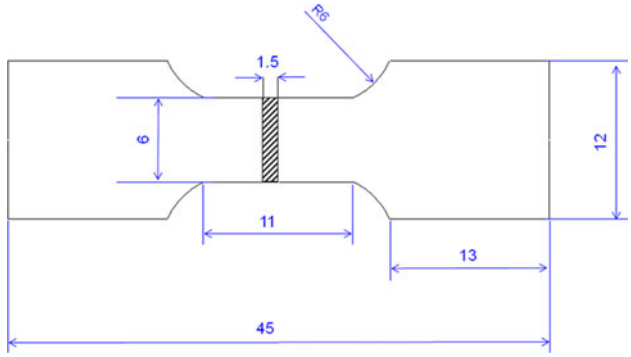

Fig. 3 Diagrammatic sketch showing dimension of tensile specimen

samples were produced by wire-electrode cutting, and the dimension of tensile specimen is shown in Fig. 3. The tensile strengths were measured by Zwick/Roell Corporation Germany) with the loading rate of 2 mm/min. SLM specimens for metallographic examinations were cut from side view, and pre-grinding was conducted with SiC sandpaper to 800 grit finish. After plane grinding, polishing was done for the samples with Cr_2O_3 suspensions on woven synthetic pads. Then, the polished sample was rinsed using distilled water to wipe off any impurities on the polished surface. Aqua fortis was used as a corrosive agent. Metallographic structure of the sample was analyzed with an Axiovert 200MAT Metallurgical Microscopy.

3. Results

To make clear the influence of scan speed on the melting condition during SLM process, experiments for single line scanning on stainless steel substrate with a powder layer thickness of 0.06 mm were conducted using different scan speeds. Figure 4 shows the transverse section of laser-molten tracks produced through various scan speeds. It can be seen that, with the increase of scan speed, the molten pool size is gradually decreased. In other words, the melting track width and laser penetration depth are reduced. In addition, the wetting angle between molten pool and substrate is increased, showing a more inferiors wetting ability which is liable for pores' generation. Moreover, it should be noted that the deteriorative wetting condition tends to form many separate spheres, which is usually termed as "balling effect."

For the purpose of understanding the influence of scan speed on the density of SLM-prepared parts, SLM experiment was performed for creating separate samples with different scan speeds. It can be found that an increasing scan speed induces a higher porosity, as is presented in Fig. 5. Under a scan speed of 90 mm/s, a high density of 96% theoretical density was obtained. When scan speed was enhanced to 180 mm/s, the as-received density was decreased to 65%. In all, the density of SLM-produced parts is highly dependent on scan speed, through which controlling the porosity is possible.

It is known that mechanical performance of a part is an essential parameter for assessment of its final practicability. Based on this requirement, tensile strengths of individual samples prepared by different scan speeds were tested, as is shown in Fig. 6. It reveals that the tensile strength is also

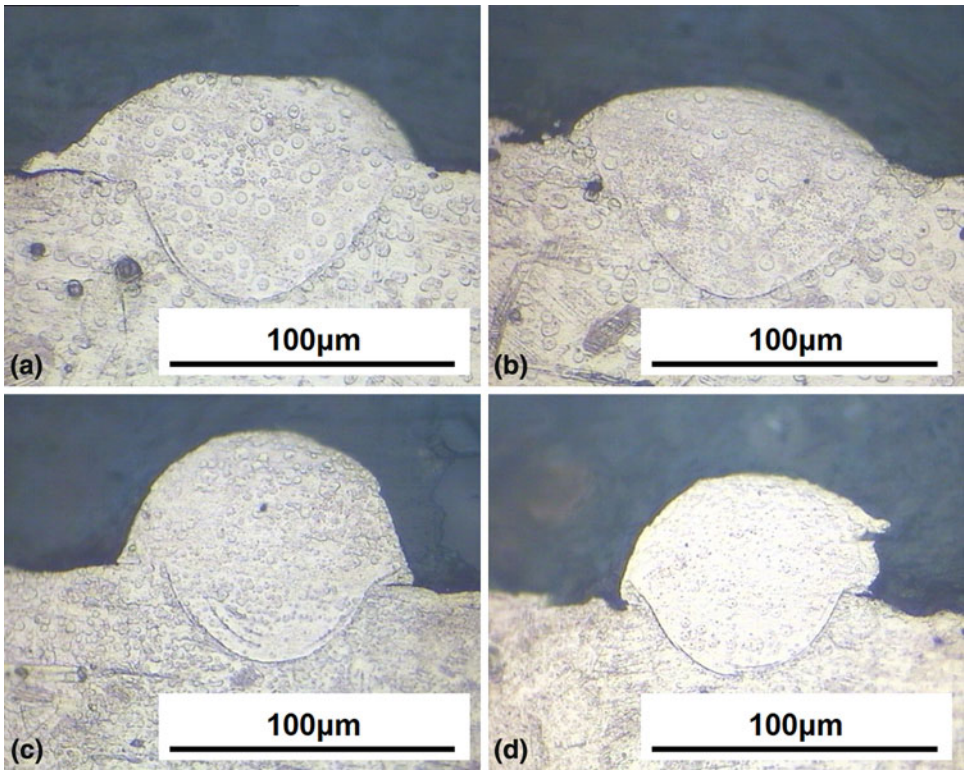

Fig. 4 Metallographs showing transverse section of laser-molten tracks produced through different scan speeds. (a) 90 mm/s; (b) 120 mm/s; (c) 150 mm/s; and (d) 180 mm/s

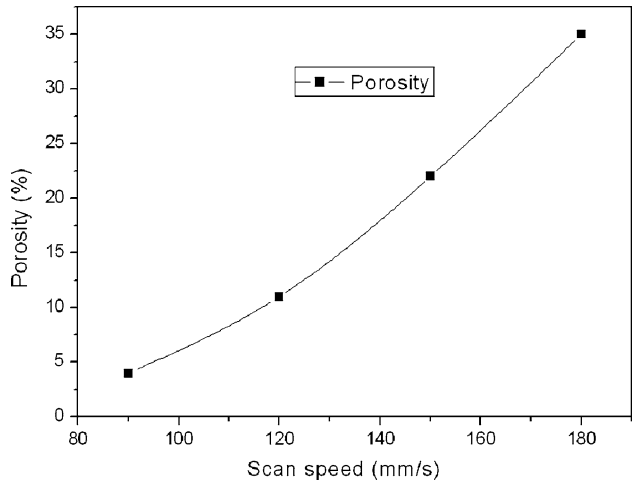

Fig. 5 Effect of scan speed on porosity of SLM-prepared 316L stainless steel samples

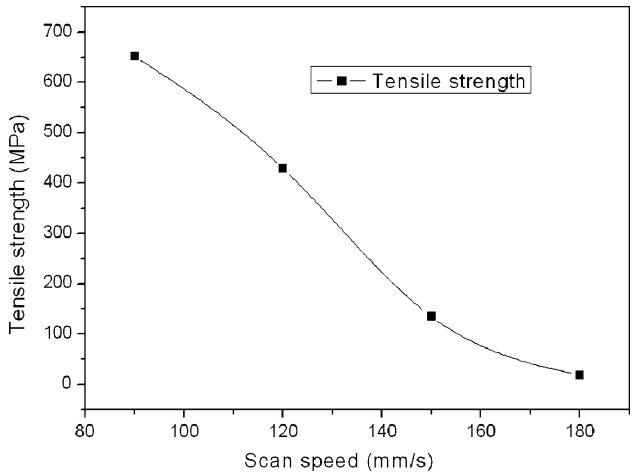

Fig. 6 Effect of scan speed on tensile strength of SLM-prepared 316L stainless steel samples

markedly influenced by scan speed, increasing of which could enable a significant decrement in tensile strength. Combined with the porosity results, it can reasonably be concluded that the final density and tensile strength of SLM-produced parts relied on scan speed. Thus, in each SLM slice layer, when scan speed is varied along a certain gradient direction, the porosity may also be varied, forming a gradient porosity structure.

Based on the above-obtained results, in every SLM layer, scan speed was varied from lower to higher along a gradient direction. SLM experiment for fabrication of gradient sample was conducted. Figure 7 presents a few typical metallographs along the gradient direction, showing irregular pore shapes without any addition of special pore-forming agents. However, it can be seen that a true gradient microstructure with relatively continuous changes in porosity was formed. Moreover, the pore size is also increased with the increasing scan speed. Therefore, the increasing scan speed can lead to a higher porosity and a smaller molten pool size. Thus, the 316L stainless steel material with a gradient porosity was developed using the SLM technique. It can be concluded that 316L stainless steel

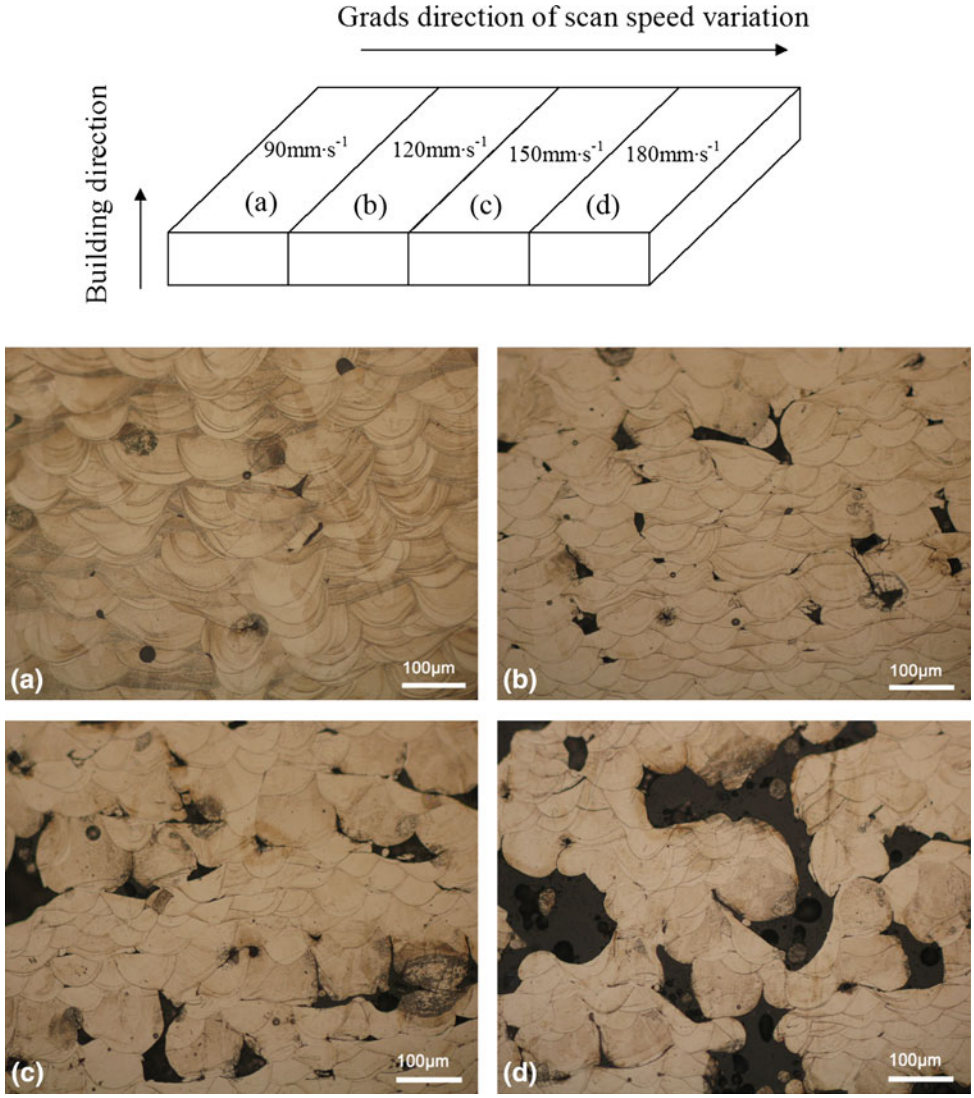

Fig. 7 Metallographs showing the porosities variation in gradient speeds direction

with porosity gradient is obtainable through a gradient change of laser scan speed.

4. Discussion

During SLM process, the powder bed is irradiated by the fiber laser beam and simultaneously the powder particles absorb the laser-induced energy by bulk coupling and powder coupling mechanism (Ref 14). Then, the temperature of powder particles is elevated rapidly under the action of absorbed energy, causing a molten pool. An extremely large temperature gradient is liable to be generated between the center and border of the molten pool, due to an applied Gaussian heat resource. Thus, the surface tension gradient and relevant Marangoni convection are formed by the effect of temperature gradient (Ref 15). Subsequently, the molten pool flow and attendant wetting are propelled under the action of capillary forces which is caused by Marangoni (Ref 16, 17). Therefore, in SLM process, the flow, spreading, and wetting of molten pool under the action of capillary forces are significantly important characteristics which need to be carefully investigated and controlled so as to obtain a required structure. The single tracks tests, shown in Fig. 4, indicate that an increase in the scan speed can lead to a smaller molten pool. This phenomenon can be understood by considering the melting temperature and attendant heat effect zone, which is caused by laser energy. Increasing scan speed with other parameters fixed as constants will result in a lower melting temperature and, accordingly, a smaller amount of liquid formation, as evidenced in a smaller molten pool size (Fig. 4). Consequently, different scan speeds could produce varied dimension levels of molten pool in cross-section view. It should be noted that the varied molten pool size could yield different pore characteristics under a fixed scan interval and layer thickness. In addition, a decreasing temperature under a high scan speed tends to cause a more bellied shape of molten pool, showing an inferior wetting condition and a much higher wetting angle between the liquid and solid phases. This can be ascribed to an increased viscosity with increasing scan speed. Under the decreased temperature in molten pool, the viscosity is relatively high, inhibiting the liquid flow characteristic. Moreover, a lower temperature cannot enable the full melting of powder particles, causing

a much smaller liquid phase volume in solid-liquid coexisting state. Therefore, the much higher volume fraction of solid phase is ultimately apt to hinder the molten pool flow, spreading, and wetting. Above all, it is obvious that the melting condition is considerably influenced by scan speed in single line scan test.

When building a three-dimensional (3D) sample, the scan tracks are arrayed line-by-line and bonded together in each slice layer. According to the same principle, a next slice layer is produced, strongly bonding the previously fabricated layer. In this situation, the scan speed influences the size, shape, and wetting of molten pool, and accordingly, determining the multi-layers forming condition and attendant pore formation. First, the formation of gradient porosity can be understood by considering the combination of geometry shape of molten pool. Figure 8 shows the diagrammatic sketch of gradient porosity formation with different scan speeds. Under a relative lower scan speed, the as-received contour outline of molten pool is big enough in size, facilitating the coherent combination of contour outline of molten pool. Thus, a structure with a low porosity tends to be formed, as illustrated in Fig. 8(a). According to obtained results, with the increase of scan speed, the contour outline size of molten pool will turn into a relatively smaller one. In this instance, when the multi-layers processing is carried out by increasing scan speed with other parameters (laser power, scan interval, and layer thickness) fixed as constants, the contour outline size will be not be large enough to completely fill the gaps. This subsequently results in a higher porosity, as is illustrated in Fig. 8(b). Moreover, the further increase of scan speed tends to cause a much smaller molten pool size, which in turn favors the increase of porosity and induces the enlargement of pore size (Fig. 8c, d). Meanwhile, the increased porosity tends to cause a decreased tensile strength. Under this circumstance, a sample with gradient porosity can be obtained by controlling scan speed with a gradient variation. It should be noted that the variation law of porosity versus scan speed in this study is in accordance with the previously reported results (Ref 8-11). Based on this point, this study made an improvisation which gives the possibility of creating a sample with gradient porosity. On the other hand, the formation of gradient porosity is ascribed to the variation of viscosity in molten pool. According to the obtained results, an increasing scan speed can lead to a higher viscosity. In the process of building a 3D part, the increasing viscosity yields worse rheological properties of molten liquid, obstructing the liquid phase from filling the pores; on the contrary, a large number of pores and metal balls would be generated due to limited liquid phase volume and a worse flow property. The combined influence of the above two factors cause the porosity and tensile strength with gradient variations.

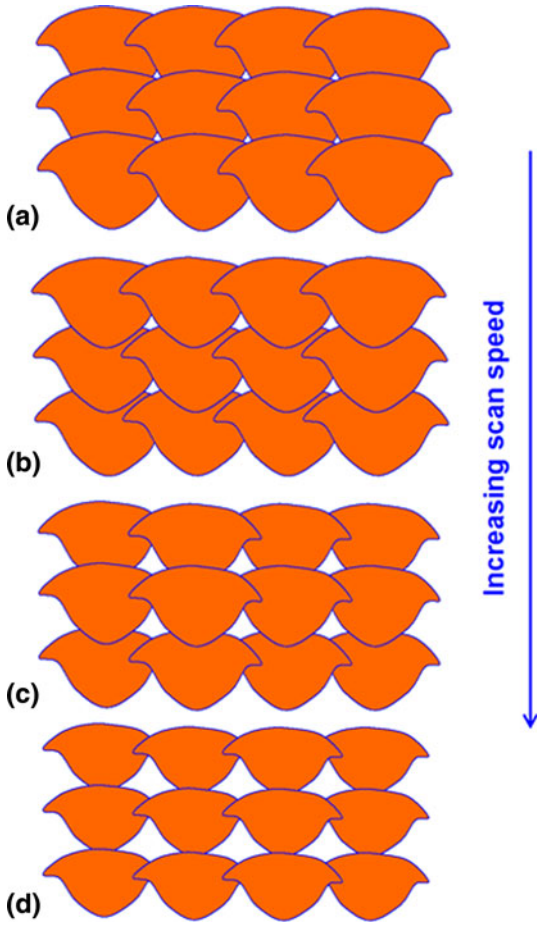

Fig. 8 Diagrammatic sketch showing pores' formation under different scan speeds

However, the variation of porosity with scan speed in this study shows an opposite trend with the literature reported by Gu et al. (Ref 13). Their work showed a drop in porosity with the increase of scan speed in the process of fabricating porous stainless steel with controllable microcellular features. The reason for the opposite trend can be understood by comparing the pores formation mechanisms. In the work by Gu et al., H_3BO_3 and KBF_4 were added into the powder system, inducing several chemical reactions with the formation of H_2O and $(BOF)_3$ in gas phase. Therefore, the additive materials in their investigation produced a sufficient amount of gas phase to favor pore formation (Ref 13). When a higher scan speed was applied for creating porous sample, the duration of laser beam at irradiating zone was decreased. Thus, the time for growth of bubble nuclei was insufficient and the bubble growth process was also inhibited, causing a decrease of porosity at a high scan speed. Consequently, in this study, the formation mechanism of pores is different from the Gu et al.'s study with additive materials generating gas phase.

Above all, setting scan speed with a gradient variation enables a gradient-varied molten pool, accordingly, an interesting gradient porosity structure. The results presented in Fig. 7 reflects a trend in porosity variation in the 316L stainless steel part, suggesting that the porosity of SLM-fabricated part could be effectively controlled by varying scan speeds. This technique can be used for many practical applications, such as for biomaterials. It is known that the tissue cell growth is favored with a high porosity; however, the high porosity can decrease its mechanical property. Thus, for an artificial bone biomaterial, a gradient porosity metal with highly controllable porosity is a requisite.

5. Conclusion

SLM technique was demonstrated to be a feasible method for building a pore gradient 316L stainless steel material. The melting characteristics of single track show a high correlativity

with scan speed, which can be reflected by a decreased molten pool size coupled with a worsened wetting ability with an increased scan speed. Moreover, the density and tensile property of SLM sample are also dependent on scan speed. Therefore, the variation of porosity from lower to higher could be effectively achieved by increasing scan speed. Thus, by setting a gradient variation scan speed in each SLM layer, a 316L stainless steel sample with a gradient porous microstructure along speed gradient direction can be fabricated, due to the variational melting condition. Overall, SLM enables the fabrication of pore gradient 316L stainless steel parts, and many other alloys. The introduction of SLM indicates a new direction for fabricating pore gradient metals.

Acknowledgments

The authors gratefully appreciate the financial supports from the National High-Tech Program (863) of China (2007AA03Z115), Independent fund of State Key Laboratory of Material Processing and Die & Mould Technology of Huazhong University of Science & Technology (HUST) and Open fund of State Key Laboratory of Powder Metallurgy of Central South University (2008112022). The authors also thank the Analytic and Testing Center of HUST.

References

1. J. Banhart, Manufacture, Characterisation and Application of Cellular Metals and Metal Foams, *Prog. Mater. Sci.*, 2001, **46**(6), p 559–632
2. Y.P. Zhang, D.S. Li, and X.P. Zhang, Gradient Porosity and Large Pore Size NiTi Shape Memory Alloys, *Scripta Mater.*, 2007, **57**, p 1020–1023
3. F.R. Cichocki, K.P. Trumble, and J. Rodel, Tailored Porosity Gradients via Colloidal Infiltration of Compression-Molded Sponges, Presented at *99th Annual Meeting of the American-Ceramic-Society*, May 4–7, 1997 (Cincinnati, OH), 1997
4. R. Clasen and J. Tabellion, Electric-Field-Assisted Processing of Ceramic—Part 1: Perspectives and Applications, *CFI Ceram. Forum Int.*, 2003, **80**(10), p 40–45
5. K. Nishiyabu, S. Matsuzaki, K. Okubo, M. Ishida, and S. Tanaka, Porous Graded Materials by Stacked Metal Powder Hot-Press Moulding, Presented at *8th International Symposium on Multifunctional and Functionally Graded Materials (FMG2004)*, July 11–14, 2004 (Leuven, Belgium), 2004
6. E.C. Santos, M. Shiomi, K. Osakada, and T. Laoui, Rapid Manufacturing of Metal Components by Laser Forming, *Int. J. Mach. Tools Manuf.*, 2006, **46**(12–13), p 1459–1468
7. D.D. Gu and Y.F. Shen, Effects of Dispersion Technique and Component Ratio on Densification and Microstructure of Multi-Component Cu-Based Metal Powder in Direct Laser Sintering, *J. Mater. Process. Technol.*, 2007, **182**, p 564–573
8. J. Dutta Majumdar, A. Pinkerton, Z. Liu, I. Manna, and L. Li, Microstructure Characterisation and Process Optimization of Laser Assisted Rapid Fabrication of 316L Stainless Steel, *Appl. Surf. Sci.*, 2005, **247**, p 320–327
9. A. Simchi, Direct Laser Sintering of Metal Powders: Mechanism, Kinetics and Microstructural Features, *Mater. Sci. Eng. A Struct. Mater. Prop. Microstruct. Process.*, 2006, **428**, p 148–158
10. D.D. Gu, Y.F. Shen, J.L. Yang, and Y. Wang, Effects of Processing Parameters on Direct Laser Sintering of Multicomponent Cu Based Metal Powder, *Mater. Sci. Technol.*, 2006, **22**(12), p 1449–1455
11. A. Simchi and H. Pohl, Effects of Laser Sintering Processing Parameters on the Microstructure and Densification of Iron Powder, *Mater. Sci. Eng. A Struct. Mater. Prop. Microstruct. Process.*, 2003, **359**, p 119–128
12. D.D. Gu and Y.F. Shen, Processing Conditions and Microstructural Features of Porous 316L Stainless Steel Components by DMLS, *Appl. Surf. Sci.*, 2008, **255**, p 1880–1887
13. Y.F. Shen, D.D. Gu, and P. Wu, Development of Porous 316L Stainless Steel with Controllable Microcellular Features Using Selective Laser Melting, *Mater. Sci. Technol.*, 2008, **24**, p 1501–1505
14. P. Fischer, V. Romano, H.P. Weber, N.P. Karapatis, E. Boillat, and R. Glardon, Sintering of Commercially Pure Titanium Powder with a Nd:YAG Laser Source, *Acta Mater.*, 2003, **51**, p 1651–1662
15. H.J. Niu and I.T.H. Chang, Selective Laser Sintering of Gas and Water Atomized High Speed Steel Powders, *Scripta Mater.*, 1999, **41**, p 25–30
16. D.D. Gu and Y.F. Shen, Effects of Processing Parameters on Consolidation and Microstructure of W–Cu Components by DMLS, *J. Alloys Compd.*, 2009, **473**, p 107–115
17. D.D. Gu and Y.F. Shen, Influence of Cu-Liquid Content on Densification and Microstructure of Direct Laser Sintered Submicron W-Cu/Micron Cu Powder Mixture, *Mater. Sci. Eng. A Struct. Mater. Prop. Microstruct. Process.*, 2008, **489**, p 169–177